JOURNAL OF OPTOELECTRONICS AND ADVANCED MATERIALS Vol. 10, No. 6, June 2008, p. 1384 - 1389

Characteristics of electrochemically obtained $Ni_{96.7}Mo_{3.3}$ alloy powder

L. RIBIĆ-ZELENOVIĆ, M. SPASOJEVIĆ, A. MARIČIĆ*, M.RISTIĆ[a]
Joint Laboratory for Advanced Materials of Serbian Academy of Science and Arts, Section for Amorphous Systems, Svetog Save 65, 32000 Cacak, Serbia
[a]Serbian Academy of Science and Arts Belgrade, Serbia

Nickel molybdenum alloy powder was obtained by electrochemical deposition of a solution of 0.035 mol dm^{-3} $NiSO_4 \cdot 7H_2O$; 0.007 mol dm^{-3} $Na_2MoO_4 \cdot 2H_2O$; 0.007 mol dm^{-3} NaCl and 0.7 mol dm^{-3} NH_4OH on a titanium cathode with a current density of j=100 mA cm^{-2}. X-ray analysis established that the powder consisted of 20% amorphous and 80% crystalline teseral phase of a solid solution of the $Ni_{96.7}Mo_{3.3}$ alloy. The amorphous phase forms a matrix hosting *FCC* phase nanocrystals with an average dimension of 18 nm. It was established that molybdenum atoms increase the minimal density of randomly distributed dislocations and mean microstrain values and impede formation of new nucleuses and thus accelerate formation of the alloys' amorphous phase. Powder particles were not spherical but elongated. The maximal particle length varied between 7 and 30 μm, while the minimal was between 3.5 and 17 μm. SEM micrographs show two particle shapes: larger particles with a cauliflower shape and smaller particles with a dendrite shape. Based on EDS spectra it was established that cauliflower shaped particles contained on average 30% more molybdenum than dendrite shaped particles. X-ray photoelectron spectroscopy showed that the chemical composition of the surface particle layer differed from the bulk particle composition. The surface layer consisted of adsorbed water molecules. OH groups are below this layer followed by Ni_2O_3 oxides and MoO_3.

(Received December 21, 2007; accepted June 4, 2008)

Keywords: Amorphous powder, Nickel and molybdenum alloy, Nanocrystals, Dendrites

1. Introduction

Technical progress and development of new technologies is significantly accelerated with the development of new materials. Nanostructured materials are widely applied, due to their specific electric, magnetic, corrosive and other properties [1-16]. In the last few decades new materials were often obtained by powder sintering. Powders with specific properties can be obtained by electro-chemical deposition [8, 16-26]. Properties of powders obtained electrochemically and those with the same chemical composition obtained using other methods usually differ. A suitable selection of the solution composition, temperature and movement rate, cathode nature, distance between electrodes and current density results in obtaining of powders with set, specific characteristics [8, 16-26]. The deposition current density significantly influences the deposit nature. Coatings are formed for current densities lower than the boundary diffusion current. Crystal powders form for the boundary diffusion current, while nanocrystals and amorphous powders form for significantly higher overvoltage [8, 16-26].

Nanostructure Ni and Mo alloys are widely applied due to their specific electric, magnetic and other properties, high corrosion and thermal stability and high catalytic activity for electrochemical evolution of hydrogen and anodic evolution of oxygen [23,25, 26-31]. Nickel and molybdenum alloys obtained by the metallurgical procedure are expensive due to the high melting point of molybdenum. However, nickel and molybdenum alloys can be obtained by electrodeposition from water solutions [23, 25, 26, 31-45].

In this paper chemical, structural and morphological characteristics of the electrochemically obtained $Ni_{96.7}Mo_{3.3}$ alloy were investigated.

2. Experimental

Electrochemical deposition of $Ni_{96.7}Mo_{3.3}$ powder was performed in a glass electrochemical cell with a volume of 2 dm^3 with a special part for a Lugin capillary in which a saturated calomel electrode was placed. The anode was a platinum plate with a surface of 8 cm^2, while the cathode was a titanium plate with a surface of 4.5 cm^2. The cell was in a thermostat. The working temperature was 298 ± 1K. The solution was prepared from p.a. chemicals (Merck) and water distilled three times. The solution composition was 0.035 mol dm^{-3} $NiSO_4 \cdot 7H_2O$; 0.007 mol dm^{-3} $Na_2MoO_4 \cdot 2H_2O$; 0.007 mol dm^{-3} NaCl and 0.7 mol dm^{-3} NH_4OH. The solution pH was maintained between 11.0 and 11.5 by adding ammonium solution during electrolysis.

A standard electrical circuit consisting of a programmer with a potentiostat (RDE 3 POTENTIOSTAT Pine Instrument So. Grove city. Pennsylvania), digital voltmeters (Pro's Kit 03-9303C) and an electrochemical cell were used for electrochemical measurements.

$Ni_{96.7}Mo_{3.3}$ powder was obtained by galvanostatic deposition with a current density of j = 100 mA cm^{-2}. After electrolysis the obtained powder was rinsed several times with distilled water and then with a 0.1% solution of benzene acid. After rinsing the powder was dried at 360 K.

The chemical composition of the powder obtained was determined on a PEKTAR-A.A.200-VARIAN atomic absorber.

X-ray diffraction (XRD) was recorded on a Philips PW 1710 diffractometer with CuK_α (α = 0,154 nm) radiation and a graphite monochromator. XRD data were collected with a step mode of 0.03º and collection time of 1.5 s/step. Scanning electron microscopy (SEM) was conducted with a JEOL.JSM 5300 equipped with an EDS-QX·2000S spectrometer.

X-ray photoelectron spectroscopy (XPS) experiments were carried out using a ''SERIES 800 XPS'' Kratos Analytical device. The Mg K_α line at 1253.6 eV was used for excitation in all cases. During experiments the vacuum in the analytic camera was at the level of $1{,}33 \cdot 10^{-7}$ Pa. The allowed energy determined as the width of the half-height of the Ag $3d_{3/5}$ peak was 1.2 eV. The accuracy of bond energy determination was ≤0.1 eV. All measurements were referenced to the C 1s line binding energy of 285.0 eV.

Analysis of the size and shape of powder particles was performed using a Leica Q 500 MC automatic device for microstructural analysis.

3. Results and discussion

The atomic absorption method was used to determine that the electrochemically obtained nickel and molybdenum powder alloy had the composition $Ni_{96.7}Mo_{3.3}$.

The phase structure of the powder was determined using X-ray analysis. Based on measured intensities and positions of diffraction maximums and the JCPD standard, crystal phases were identified and unit cell parameters and microstructure parameters were determined.

Based on the X-ray diagram presented in Fig.1. it was established that the $Ni_{96.7}Mo_{3.3}$ powder consisted of only one crystal solid solution teseral phase whose structure is described by space group Fm-3m.

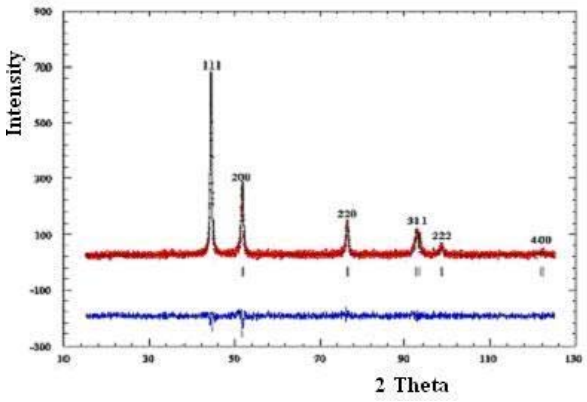

Fig.1. Rietveld's diagram for $Ni_{96.7}Mo_{3.3}$ alloy powder.

The point curve in Fig. 1. represents the measured values. The top full line shows calculated values for the structural model. The bottom full line represents the difference between measured and calculated values. The vertical lines below the top curves represent positions of Bragg reflections for different *FCC* phase planes.

Four well defined and two weak peaks can be noted on the diffractogram for different planes of the face-centered cubic lattice, *FCC*, of crystals of the solid solution of nickel and molybdenum ($Ni_{96.7}Mo_{3.3}$ alloy). Parameters of the unit cell of the FCC phase are: a=0.3254(2) nm, α=90º and V=0.043815(4) nm^3. The following values were obtained for microstructure parameters of the FCC phase: mean value of crystallite dimensions is 18.0 nm; mean microstrain value is $1.9 \cdot 10^{-3}$ and minimal density of randomly distributed dislocations is $8.7 \cdot 10^{11}$ cm^{-2}.

Fig.2. and Fig.3. represent the dimensional distribution of crystallites (Fig. 2.) and the dependence of the mean square root of microstrain on the distance (Fig. 3.) determined for orientation (111) using the Warren-Averbach method.

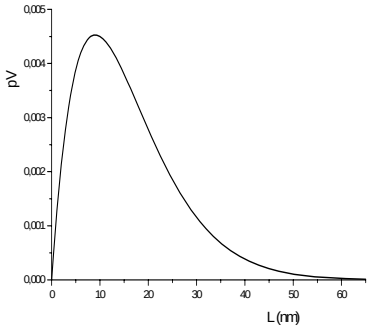

Fig.2. Dimensional crystallite distribution for $Ni_{96.7}Mo_{3.3}$ alloy powder.

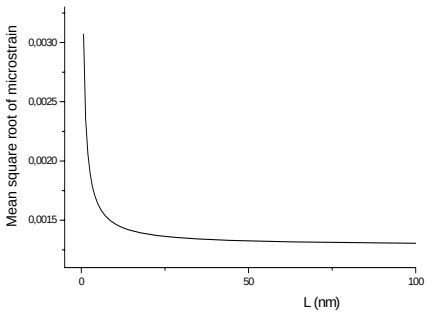

Fig.3. Mean square root of microstrain as a function of distance for $Ni_{96.7}Mo_{3.3}$ alloy powder .

Fig.2. shows that the crystallite size varies between 0.0 and 50 nm. The Rietveld method [45] was used to determine that the powder contained about 20% of an amorphous phase. Based on the results of X-ray investigations it can be supposed that the amorphous powder component makes a matrix (skeleton) in which nanocrystals are situated, i.e. the boundary between

nanocrystals consists of disordered atoms representing the amorphous phase. Confirmation that the boundary between crystals consists of several disordered atoms is: a relatively high minimal density of randomly distributed dislocations, large mean microstrain value and the obtained dependence of the mean square root of the microstrain on the distance (Fig.3).

A pure nickel deposit obtained for the same current density in the bath without the presence of Na_2MoO_4 consists of significantly larger crystalline grains with a significantly lower minimal density of randomly distributed dislocations. This indicates that molybdenum atoms impede formation of $Ni_{96.7}Mo_{3.3}$ alloy nucleuses and thus increase participation of the amorphous phase, minimal density of randomly distributed dislocations and the mean microstrain value. It has been shown that the granulometric composition and particle shape of nickel and molybdenum alloy powders depends on the deposition current density and molybdenum content [22]. The granulometric composition and particle shapes of $Ni_{96.7}Mo_{3.3}$ alloy powder is illustrated in the diagrams given in Fig. 4.

The diagrams presented in Fig. 4(a) and 4(b) show that the particles do not have a spherical shape, but are elongated. The minimal powder particle length is on average twice smaller than the maximal one.

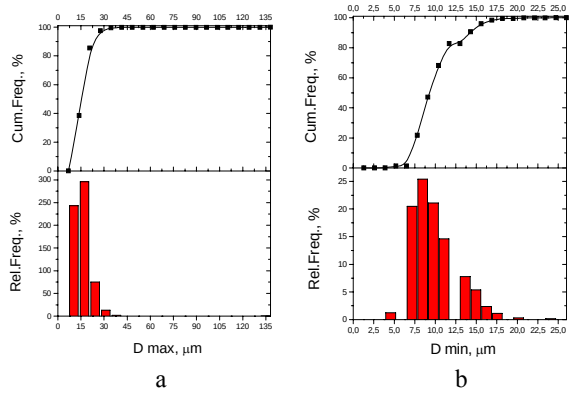

Fig.4. Cumulative D_{max} particle size distribution curves and histograms of the relative D_{max} particle size frequency distribution (a) and cumulative D_{min} particle size distribution curves and histograms of the relative D_{min} particle size frequency distribution (b) of powder particles of the $Ni_{96.7}Mo_{3.3}$ alloy.

SEM micrographs show that electrochemical deposition for j = 100 mA cm^{-2} resulted in the formation of two shapes of powder particles of the $Ni_{96.7}Mo_{3.3}$ alloy: larger particles of a cauliflower shape and smaller particles with a dendrite shape. Dendrites formed on the surface of cauliflower shaped particles (Fig.5. and Fig.6). The formed dendrites had secondary branches and higher order branches (Fig.7). Fig.5. shows a particle on which dendrite formation has started (dendrites are paler).

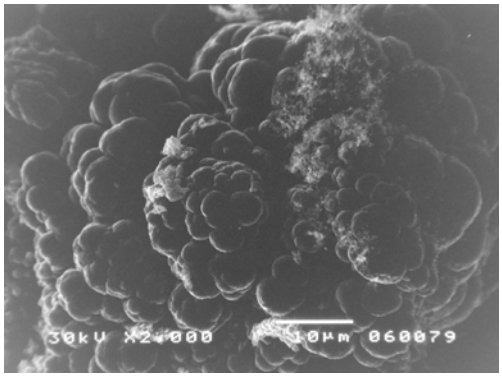

Fig.5. SEM micrograph of $Ni_{96.7}Mo_{3.3}$ alloy powder.

Fig.6. shows a particle that started growth as a dendrite and during electrolysis turned into a cauliflower at the top.

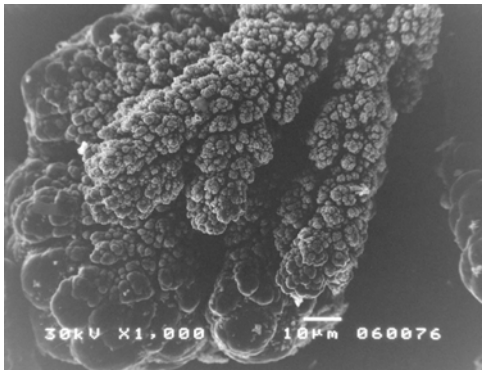

Fig.6. SEM micrograph of $Ni_{96.7}Mo_{3.3}$ alloy powder.

Fig.7. shows formed dendrites with secondary branches and higher order branches.

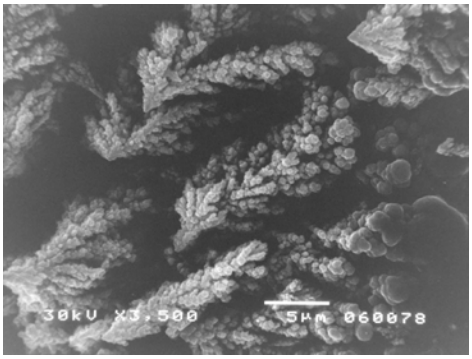

Fig.7. SEM micrograph of $Ni_{96.7}Mo_{3.3}$ alloy powder.

Based on a semi-quantitative analysis of EDS spectra of $Ni_{96.7}Mo_{3.3}$ alloy powder it has been established that cauliflower shaped particles do not have the same composition as dendrite shaped particles. Dendrites contained less molybdenum than cauliflower shaped particles. The EDS spectrum of the $Ni_{96.7}Mo_{3.3}$ alloy

powder for dendrites is given on Fig.8. and for cauliflower particles on Fig. 9, respectively.

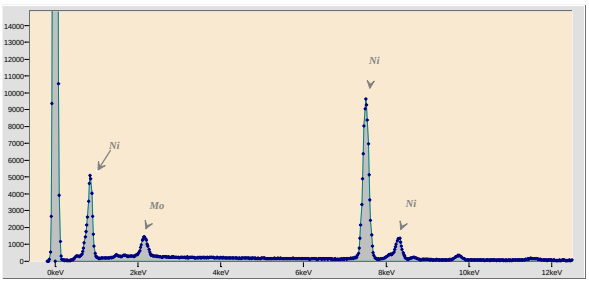

Fig.8. EDS spectrum for dendrite particles of the $Ni_{96.7}Mo_{3.3}$ alloy.

Based on the EDS spectra given in Fig.8. and Fig.9 it has been established that cauliflower shaped particles have on average 35% more molybdenum than dendrite particles. This fact shows that molybdenum particles impede formation of $Ni_{96.7}Mo_{3.3}$ alloy nucleuses.

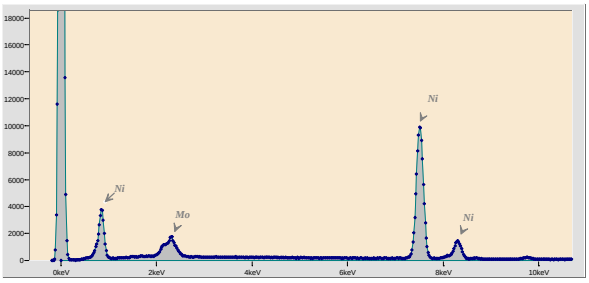

Fig.9. EDS spectrum for cauliflower shaped particles of the $Ni_{96.7}Mo_{3.3}$ alloy

X-ray photoelectronic spectroscopy (XPS) established that the chemical composition of the surface particle layer, about 10 nm thick, differed from the chemical composition of bulk powder particles of the $Ni_{96.7}Mo_{3.3}$ alloy. Fig.10, Fig.11. and Fig.12. give the spectra for Mo $3d_{5/2}$, Ni $2p_{3/2}$ and O 1s electrons of the $Ni_{96.7}Mo_{3.3}$ alloy powder.

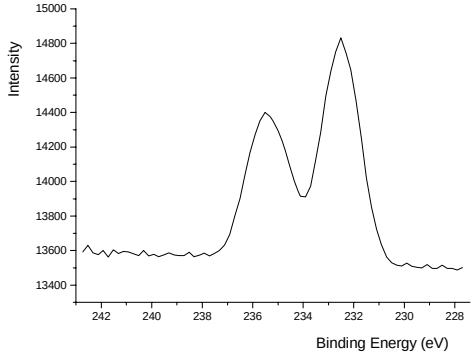

Fig. 10. XPS spectrum for Mo $3d_{5/2}$ electrons of $Ni_{96.7}Mo_{3.3}$ alloy powder.

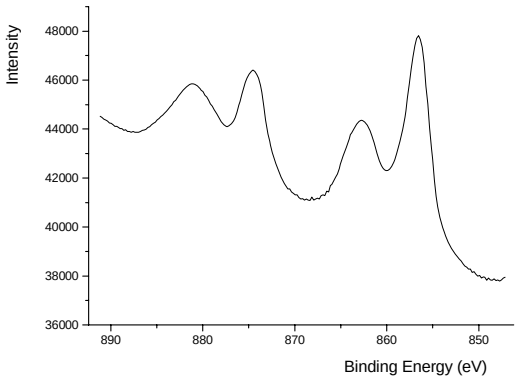

Fig.11. XPS spectrum for Ni $2p_{3/2}$ electrons of $Ni_{96.7}Mo_{3.3}$ alloy powder.

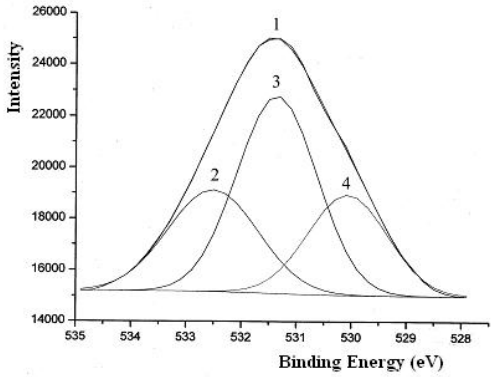

Fig.12. XPS spectrum for O 1s electrons of $Ni_{96.7}Mo_{3.3}$ alloy powder (curve 1) and O 1s electrons in molecules: H_2O (curve 2); OH group (curve 3) and Ni_2O_3 (curve 4).

Based on XPS spectra presented in figures 10, 11 and 12 bond energies of Mo $3d_{5/2}$, Ni $2p_{3/2}$ and O 1s electrons of the $Ni_{96.7}Mo_{3.3}$ alloy were determined. The values obtained are given in table 1.

Table 1. Bond energies of ni $2p_{3/2}$, mo $3d_{5/2}$ and o1s electrons.

Mo $3d_{5/2}$ (eV)	856.5
Ni $2p_{3/2}$ (eV)	232.5
O 1s (eV)	532.4-531.4 530.5

The bond energy of $2p_{3/2}$ nickel electrons corresponds to the Ni_2O_3 oxide, while the bond energy of $3d_{5/2}$ molybdenum electrons corresponds to the MoO_3 oxide. This indicates that these oxides are present in the surface layer of electrochemically obtained $Ni_{96.7}Mo_{3.3}$ alloy powder at j = 100 mA cm^{-2}.

The XPS spectrum for O 1s consists of a wide peak (Fig.12, curve 1) that is probably the result of overlapping of three peaks for O 1s electrons of the H_2O molecule (curve 2); OH group (curve 3) and Ni_2O_3 (curve 4).

The energy region between 532.4 and 532.8 eV corresponds to the bond energy of 1s oxygen electrons in

the H_2O molecule that was probably adsorbed on the powder surface. OH groups whose bond energy values of O 1s electrons are between 531.4 and 531.6 eV lie below the layer of H_2O molecules. Oxygen in nickel oxide is below the OH group layer with bond energy of 1s electrons between 530.4 and 530.5 eV.

4. Conclusion

Nickel and molybdenum alloy powder with the composition of $Ni_{96.7}Mo_{3.3}$ was obtained by electrochemical deposition from a 0.035 mol dm^{-3} $NiSO_4 \cdot 7H_2O$; 0.007 mol dm^{-3} $Na_2MoO_4 \cdot 2H_2O$; 0.007 mol dm^{-3} NaCl and 0.7 mol dm^{-3}NaOH solution at a current density of j = 100 mA cm^{-2} on a titanium cathode. The powder consisted of an amorphous matrix hosting nanocrystals with a mean size of 18 nm of the *FCC* phase. Molybdenum atoms cause a high minimal density of randomly distributed dislocations and large mean microstrain value. These atoms also hinder alloy nucleus formation and accelerate formation of an amorphous matrix. Powder particles were elongated. The maximal particle length varied between 7 and 30 μm and the minimal one between 3.5 and 17 μm. The powder consisted of two morphological particle shapes: larger particles had a cauliflower shape and smaller particles a dendrite one. Cauliflower shaped particles contained on average 35% more molybdenum that the dendrite shaped ones. The surface layer of powder particles about 10 nm thick did not have the same composition as the bulk particles. Adsorbed H_2O molecules are on the surface. OH groups are below the adsorbed layer and then Ni_2O_3 and MoO_3 oxides.

Acknowledgements

This work was supported by the Ministry for Science and Technology of the Republic of Serbia (Project 142011G) and by the Serbian Academy of Science and Arts (Project F-198).

References

[1] T. R. Anantharaman. Trans. Tech., Aedermansorf, Switzerland. 1948.
[2] P. Haasen, R. I. Joffe, Amorphous Metals and Semiconductors, Pergamon, London, 1986.
[3] N. F. Motte, E. A. Davis, Electronic Processes in Non-Crystalline Materials, Clarendon Press, Oxford, 1979.
[4] H. Steeb, H. Warlimont, Rapidly Quenched Metals, Elsevier, Amsterdam, 1985.
[5] Yu. A. Kunitsky, V. I. Lisov, T. L. Tsaregadskaya, O. V. Turkov, Sci Sintering. **35**, 319 (2003).
[6] L. A Jakobson, J. Mc. Kittrik, Rapid Soldification Processing, Eisevier, 1994.
[7] M. V. Sušić, J. Mat. Sci. **22**, 3011 (1987).
[8] A. Maričić, M. Spasojević, L. Rafailović, V. Milovanović, L.Ribić-Zelenović, Mater. Sci. Forum, **453**, 411 (2004).
[9] M. V. Sušić, P. V. Budberg, S. P. Allisova, A. M. Maričić, J. Serb. Chem. Soc. 60 (1995).
[10] A.M. Maričić, M.M. Ristić, Sci. Sintering, **35**, 31 (2003).
[11] M. V. Sušić, D. Minić, A. M. Maričić, B. Jordović, Sci Sintering, **28**, 105 (1996).
[12] A. M. Maričić, M. M. Ristić, Sci. Sintering **28**, 182 (1996).
[13] M. V. Sušić, A. M. Maričić, N. S. Mitrović, Sci. Sintering, **28**, 105 (1996).
[14] A. M. Maričić, M. V. Sušić, M. M. Ristić, J.Serb. Chem. Soc. **62**, 643 (1997).
[15] M. Spasojević, A. Maričić, L. Rafailović, Sci Sintering, **36**, 105 (2004).
[16] A. R. Despić, K. I. Popov, Modern Aspects of Electrodhemisty, Vol. 7 Plenum Press, New York, 1972.
[17] N. Ibl, Helv. Chim. Acta, **37**, 11 49 (1954).
[18] K. I. Poopov, M.G. Pavlović, Electrodeposition of Metal Powders with Controlled Particles Grains Size and Marphology in Modeern Aspects of Elestrochemistry, B.E. Conway, J.O.M. Bockris, R. E. White. Eds., Vol 24 Plenum, New York, 1973, pp.299-391.
[19] M. G. Pavlović, Lj. J. Pavlović, N. D. Nikolić, K. I. Popov, Mater Sci Forum, **3352**, 65 (2000).
[20] M.G.Pavlović, K.I. Poopov, E..R.Stojiković, Bull. Electrochem. **14**, 211 (1998).
[21] M. G. Pavlović, Lj. J. Pavlović, E. R. Ivanović, V.Radmilović, K.I. Poopov, J.Serb.Chem. Soc. **66**, 923 (2001).
[22] L. Ribić-Zelenović, L. Rafailović, M. Spasojević, A. Maričić, Sci Sintering, **38**, 145 (2006).
[23] S. Randjić, A. Maričić. L. Rafailović, M. Spasojević, M.M. Ristić, Sci Sintering, **38**, 139 (2006).
[24] L. Ribić-Zelenović, R. Simeunović, A. Maričić, M. Spasojević, Mater Sci Forum, **555**, 539 (2007)
[25] A.Maričić, M. Spasojević, L. Rafailović, V. Milovanović, L. Ribić-Zelenović, Mater Sci Forum **453**, 411 (2004).
[26] J. Niedbala, Acta Metall. Slovaca, **11**, 166 (2005).
[27] J. Niedbala, K. Wykpis, A. Budinck, E. Logiewka, Archives Mat. Sci. **23**, 123 (2002).
[28] E. Lagiewka, A. Budnick, J. Niedbala, Archives Mat. Sci.**23**. 2, 137 (2002).
[29] Beltowska-Lehman E., Chassqing E., J.Appl. Elecrochem. **27**, 568 (1977).
[30] Y. Zeng, S. W. Yao, X. Q. Cao, H. X. Juany, Z. Y. Zhoni, H.T. Guo, Chin. Chem. **15**, 193 (1997).
[31] J.Y. Huot, J. Electrochem. Soc., **136**, 32 (1989).
[32] I. Arul Ray, V.K.Venkatesan, Inst. Hydrogen Eneergy, **13**, 215 (1982).
[33] D. Olszak, V.K. Partony, H. Mayja, Nanostruct. Materials, **12**, 6e21 (1999).
[34] W. Z. Q. Hue, X. Zhang, Surf. Coat. Techn. **1-2**, 50 (1997).

[35] S. W. Yao, Y. Zeng. H. T. Guo, Surf. Fin. **16**, 9 (1994). (in Chinese)
[36] Y. Zeng, S. W. Yao. H. T. Guo, Platinum Surf. Fin. **16e**, 9 (1994). (in Chinese)
[37] Y. Zeng, S. W. Yao H. T. Guo, Platinum Surf Fin. **82**, 64 (1995).
[38] H. Fukusima, T. Akyama, S. Akagi, Trans. Jpn. Ins. Met. **20**, 358 (1979).
[39] E. Classaing, K. V. Quang. R. Wiart, J. Appl. Electrochem, **19**, 839 (1989).
[40] Y. Zeng, S. W. Yao, H. T. Guo, Chim. J.Chem. **15**, 193 (1997).
[41] E. J. Podlaha, D. Londolt, J. Electrochem. Soc. **143,** 855 (1996).
[42] E. J. Podlaha, D. Londolt, J. Electrochem. Soc. **144**, 1672 (1997).
[43] E. Navarro-Flores, Z. Chong, S. Omanović, J.Mol. Catal: Chem. **226**, 179 (2005).
[44] L. S. Sanches, S. H. Dominigues, C. E.B. Aarino, L. H. Mascaro, Electrochem. Comm. **6**, 543 (2004).
[45] H. Rietveld, J. Appl. Crystalogr. **2**, 65 (1969).

*Corresponding author: marec@tfc.kg.ac.yu